ANGULAR SELF-SENSING ALGORITHM FOR LORENTZ FORCE TYPE INTEGRATED MOTOR-BEARING SYSTEM

Han-Wook Jeon
freddie@novic.kaist.ac.kr

Sung-Ho Park
shpark@cwllab.kaist.ac.kr

Youngjin Park
yjpark@kaist.ac.kr

Chong-Won Lee
cwlee@novic.kaist.ac.kr

Center for Noise and Vibration Control (NOVIC), Dept. of Mechanical Eng.,
KAIST, Science Town, Daejeon, KOREA

ABSTRACT

Recently, a disk type integrated motor-bearing system using Lorentz force design principle has been developed in the laboratory. It is composed mainly of a stator with six windings and two rotor disks of eight-pole permanent magnets. One of the disadvantages of the Lorentz force type integrated motor-bearing system is that it requires an angular position sensor to perform commutation between the torque control current and the angular position of the rotor.

In this paper, an angular self-sensing algorithm is proposed and implemented to a Lorentz force type integrated motor-bearing system, so that the system can be made compact in size, light, and reliable. It is based on the principle that the flux linkages of stator windings, calculated from the voltage and torque control current, are the functions of the rotor angle. The tracking angular position error is proven to converge toward zero using the Lyapunov stability method, and the experimental results show that the initial error decays within about 4 seconds. It is found that the angle resolution of the algorithm remains about 1º over the speed range of 100 to 1000 rpm. The error sources are analyzed and experimentally identified.

Keywords: Integrated motor-bearing system, Self-sensing, Lorentz force

INTRODUCTION

Active magnetic bearing (AMB) is an electromagnetic device that supports the rotor using controlled electromagnetic forces without any contact. AMBs have been successfully used in many applications due to such advantages as free of mechanical contact and lubrication, high peripheral speed and precision operation, and adjustability of the bearing stiffness and damping within physical limits. However there still remain some problems to be addressed with AMB. One of the problems is that it requires a rather long axial shaft length to accommodate an electric motor to drive the rotor as well as AMB, lowering the flexural critical speeds. One of the solutions used to reduce the axial shaft length of motors with AMBs is to combine the motor with AMB magnetically. This combined device is called the integrated motor-bearing system (IMB), which is frequently referred to as “bearingless motor”.

Compared with motors supported by AMBs, IMBs are compact and thus advantageous to small-sized rotating systems such as artificial heart pumps [1] and hard disk drives. Recently various types of IMBs have been developed [2] and proposed including the permanent magnet type [3], reluctance type [4], inductance type [5], etc. It is common that many of these designs use the attractive force between a rotor and stator (reluctance-type force) for position control of the rotor. Recently, several papers have proposed permanent magnet IMB designs that use Lorentz-type force to produce both motoring torque and bearing forces [6-7].

In order to perform the rotational speed and radial position control, various angular position sensors such as encoders and resolvers are necessary; the angular position information is essential to accurately produce the radial control forces in the required directions. However the use of these position sensors causes problems such as reduction in reliability, increase in motor volume in the axial direction, and higher cost. To overcome these drawbacks, many efforts to realize light weight, compact permanent magnet synchronous motors (PMSM), not requiring angular position sensors, have already been reported [8]. Note here that permanent magnet IMB has a similar configuration to PMSM.

In this paper, an angular self-sensing algorithm based on flux linkage increment with respect to the angular position of a rotor [9] for Lorentz force type permanent magnet IMB is presented. Using mathematical synthesis, it is shown that the actual angular position can be achieved from the machine voltage equations for each stator winding; only the line currents and voltages are measured for the calculation of flux linkages. Furthermore, using Lyapunov stability analysis method, it is shown that the tracking angular position error converges to zero in spite of the proposed integration form of self-sensing algorithm. To verify the feasibility of the proposed method, extensive experimental tests are conducted over the speed range of 100rpm to1000rpm. It was found through experiments that the initial error decays within approximately 4 seconds and the angle resolution of the algorithm remains about 1º over the whole speed range.

1. OVERVIEW OF THE LORENTZ FORCE TYPE IMB [6]

Figure1 shows the cross-sectional view of the Lorentz force type permanent magnet IMB developed in the laboratory. The system consists mainly of two components, stator and rotors; the stator has 6 equi-spaced concentrated coreless windings and the rotor has 4 pole permanent magnets as shown in Fig. 2. A

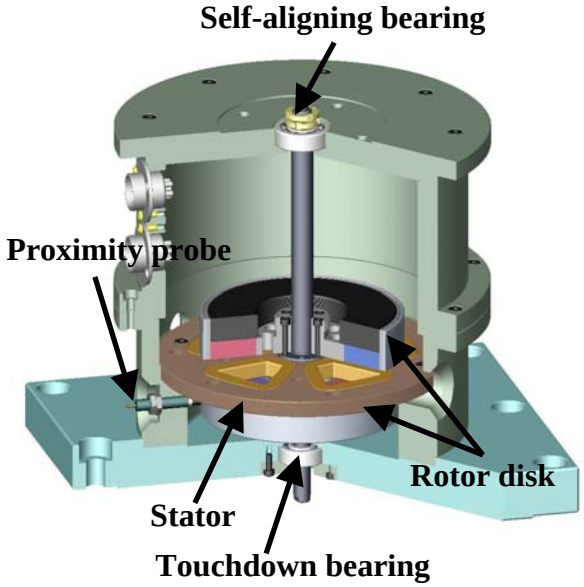

Fig.1 Cross-sectional view of IMB

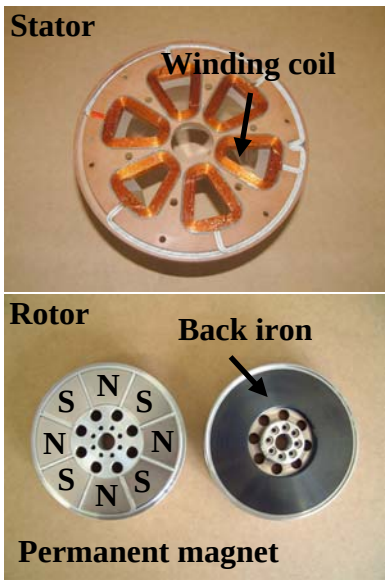

Fig. 2 Stator and Rotor of IMB

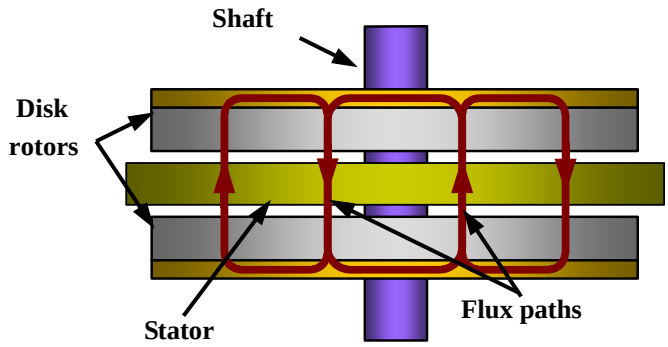

Fig.3 Flux paths of dual disk rotor configuration

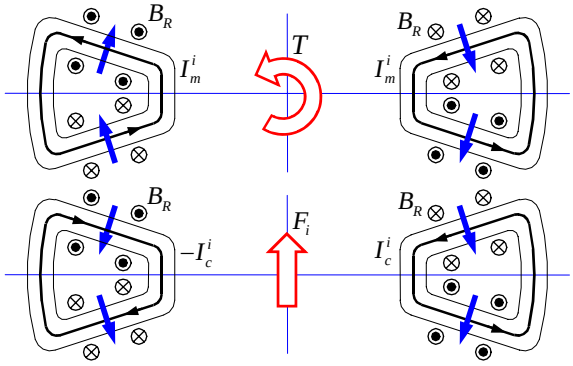

Fig.4 Generation of (a) torque and (b) radial force of IMB

pair of rotor disks is placed at both sides of a single stator disk like a sandwich. Since the opposite poles of magnets face each other as shown in Fig.3, the axial magnetic flux can pass through the stator windings.

Figure4 illustrates the basic principle of torque and radial force generation. The dots and crosses in the circles represent the magnetic flux coming out of and going into the page, respectively, and the loop in the windings indicates the current flow, with the arrow on the loop showing the current flow direction. According to the Lorentz law, electromagnetic forces, which are represented by the thick arrows, are produced in the upper and lower sides of windings for the counter-clockwise current flows in the right and left windings. The reaction forces on the rotor have the counter direction to the forces generated in the windings, resulting in a couple moment. The contour arrow at the center indicates the motoring torque. For radial force generation, the current flow in the left side winding is reversed; the resulting reaction force on the rotor will head in the upper direction. As the rotor rotates, the magnetic flux polarity alternates periodically, so the current flow must be controlled to flow synchronous to the angular position of the rotor.

2. THEORETICAL ANALYSIS OF LORENTZ FORCE TYPE IMB [6]

For the theoretical analysis of the system, magnetic flux density generated by 4 pole permanent magnets of the rotor are assumed, in the sinusoidal form, as

$$B_R = B\cos(4\theta_r - 4\theta) \qquad (1)$$

where B is the amplitude of the flux density, θ_r is the mechanical angular position of the rotor and θ is the angular coordinate.

$$I_m^i = I_M \cos(\theta_d + \psi + \frac{2}{3}\pi i) \qquad (2)$$

where θ_d is the electrical angular position of the rotor, ψ is the torque angle, I_M is the magnitude of the current, and $i = 0,1,2,3,4,5$ represents the numbering of six stator windings.

The motoring torque produced by these currents can then be obtained using the Lorentz law as

$$T = 6I_M Bkrl \sin(\frac{2}{5}\pi)\sin\psi \qquad (3)$$

where k, r, and l denote the number of turns in a concentrated winding, the effective radius of stator windings and the effective length of winding.

Similarly to the previous procedure for the generation of motoring torque, consider the currents for the radial control force, in the form of

$$I_c^i = I_C \cos(\theta_d + \phi + \frac{1}{3}\pi i) \tag{4}$$

where I_C and ϕ represent the magnitude of the current and the phase shift. We obtain the expressions for the radial control forces in the x and y directions as

$$\begin{aligned} F_x &= 3I_C Bkl \cos\phi \\ F_y &= 3I_C Bkl \sin\phi \end{aligned} \tag{5}$$

3. ANGULAR SELF-SENSING ALGORITHM

The flux linkage is defined as the amount of the flux passing through each stator winding by the permanent magnets of the rotor, which can be expressed as

$$\begin{aligned} \lambda_m^i(t) &= B_R(t) A_w \\ &= 2Bkrl \sin(\frac{2}{5}\pi) \cos(4\theta_r + \frac{2}{3}\pi i) \end{aligned} \tag{6}$$

where A_w is the effective area of stator winding facing the magnets. It can be easily realized that the flux linkage is a function of the angular position of the rotor.

When the resistances and inductances in all windings are assumed to be identical and constant, the voltage equation of each stator winding can be given by

$$v_i(t) = R\left(I_m^i(t) + I_c^i(t)\right) + L\frac{d(I_m^i(t) + I_c^i(t))}{dt} + \frac{d\lambda_m^i}{dt} \tag{7}$$

where v_i, R, and L is the voltages, resistance, and inductance of each winding, respectively. The last term, which is defined as differentiation of the flux linkage λ_m^i, is called the back electromotive force (back EMF). Hence, by differentiating equation (6), the back EMF can be obtained from

$$\frac{d\lambda_m^i}{dt} = 2Bkrl \sin(\frac{2}{5}\pi)\omega_r \cos(4\theta_r + \frac{2}{3}\pi i + \frac{\pi}{2}) \tag{8}$$

where ω_r is the rotational speed of the rotor. This equation indicates that the back EMF is proportional to the rotational speed.

As shown in the torque current equation (2), the phases of the torque currents in the ith and $(i+3)$th windings facing each other are identical, while the radial control currents have opposite phases as shown in equation (4). Therefore, by simply summing the voltage equations for the ith and $(i+3)$th windings, new voltage equation reduces to

$$\frac{v_i(t)+v_{i+3}(t)}{2} = RI_m^i(t) + L\frac{dI_m^i(t)}{dt} + \frac{d\lambda_m^i}{dt} \quad (9)$$

Letting Δt be the sampling interval, equation (9) can be transformed into

$$\left(\frac{v_i(t)+v_{i+3}(t)}{2} - RI_m^i(t)\right)\Delta t - L\Delta I_m^i(t) = \Delta\lambda_m^i \quad (10)$$

Note that the actual flux linkage increment can be obtained by calculation using the measured line voltages and currents in the stator windings at discrete time instants. Similarly to equation (10), equation (8) can be transformed into

$$\Delta\lambda_m^i = 2Bkrl\sin(\frac{2}{5}\pi)\cos(4\theta_r + \frac{2}{3}\pi i + \frac{\pi}{2})\Delta\theta_r \quad (11)$$

Comparing the actual flux linkage increment equation (10) obtained from the measurement with the analytical flux linkage increment equation (11) and rearranging the results, we obtain

$$\Delta\lambda_m^i = k_e\Delta\tilde{\theta}_r e_i(\tilde{\theta}_r) \quad (12)$$

where

$$e_i(\tilde{\theta}_r) = B\sin(\frac{2}{5}\pi)\cdot\cos(4\tilde{\theta}_r + \frac{2}{3}\pi i + \frac{\pi}{2}) \quad (13)$$

Here, $\Delta\lambda_m^i$ is the flux linkage increment of each stator winding, $k_e(=2krl)$ is the back EMF constant, $\tilde{\theta}_r$ is the estimated angular position, and $\Delta\tilde{\theta}_r$ is the increment of the estimated angular position. As shown in equation (12), for known parameters R, L, and k_e, the angular rotor position can be calculated by measuring the voltages and currents in the stator windings. However, for the angular positions where the back EMF functions vanish, it is not possible to estimate the angular position by using equation (12). To resolve this singularity problem, equation (12) can be rewritten as

$$\begin{aligned}\Delta\tilde{\theta}_r e_0(\tilde{\theta}_r) &= \frac{\Delta\lambda_m^0}{k_e}\\ \Delta\tilde{\theta}_r e_1(\tilde{\theta}_r) &= \frac{\Delta\lambda_m^1}{k_e}\\ \Delta\tilde{\theta}_r e_2(\tilde{\theta}_r) &= \frac{\Delta\lambda_m^2}{k_e}\end{aligned} \quad (14)$$

Multiplied the above three equations by $e_2(\tilde{\theta}_r)$, $e_1(\tilde{\theta}_r)$ and $e_0(\tilde{\theta}_r)$,respectively, and adding the resulting equations, we can derive the angular position increments of the rotor as

$$\Delta\tilde{\theta}_r = \frac{1}{k_e} \cdot \frac{\Delta\lambda_m^0 e_2(\tilde{\theta}_r) + \Delta\lambda_m^1 e_0(\tilde{\theta}_r) + \Delta\lambda_m^2 e_1(\tilde{\theta}_r)}{e_0(\tilde{\theta}_r)e_1(\tilde{\theta}_r) + e_1(\tilde{\theta}_r)e_2(\tilde{\theta}_r) + e_2(\tilde{\theta}_r)e_0(\tilde{\theta}_r)} \tag{15}$$

Note that, once the estimated angular position $\tilde{\theta}_r(t)$ at a specific time instant is known, then the angular position increments can be calculated from equation (15). The one-step forward angular position of the rotor is then represented by

$$\tilde{\theta}_r(t+\Delta t) = \tilde{\theta}_r(t) + \Delta\tilde{\theta}_r(t) \tag{16}$$

From equations (15) and (16), we can derive the angular position at any time instant, avoiding the singularity problem in estimation procedure.

4. LYAPUNOV STABILITY ANALYSIS

As shown in equation (16), the proposed self-sensing algorithm is inherently of an integration form. Thus it should be checked, for practicality of such algorithm, if the outputs diverge infinitely due to presence of DC components, low signal to noise ratio, and so on. In this section, we will prove that the estimated output obtained by the proposed algorithm converges to zero, using the Lyapunov stability analysis.

Assuming that an angular position error at a specific discrete instant is ε_k, we can describe the estimated angular position $\tilde{\theta}_r$ as

$$\tilde{\theta}_r = \theta_r + \varepsilon_k \tag{17}$$

We also assume that Lyapunov function candidate is the square value of error ε_k, i.e.

$$V(k) = \varepsilon_k^2 \tag{18}$$

Since the above function is positive definite, in order for the error to converge to zero, it should hold

$$\Delta V(k) = \varepsilon_{k+1}^2 - \varepsilon_k^2 < 0 \tag{19}$$

where ε_{k+1} is defined as

$$\begin{aligned} \varepsilon_{k+1} &= \varepsilon_k + \Delta\tilde{\theta}_r - \Delta\theta_r \\ &= \varepsilon_k - 2\Delta\theta_r \cos(-\frac{2}{3}\pi + 4\varepsilon_k) - \Delta\theta_r \end{aligned} \tag{20}$$

Dividing the above equation by the sampling time Δt and rearranging the result, we can express the error dynamics as

$$\dot{\varepsilon} = -\left(2\cos(-\frac{2}{3}\pi + 4\varepsilon) + 1\right)\Delta\theta_r \qquad (21)$$

From the above equation, we can find many equilibrium points including zero. But we consider only the equilibrium point at zero, implying that the estimation error is allowed to converge to zero. From equation (15) and (19), we can derive

$$\begin{aligned}\Delta V(k) = -\Delta\theta_r &\left\{2\cos(-\frac{2}{3}\pi + 4\varepsilon_k) + 1\right\} \\ \times &\left\{2\varepsilon_k - \left(2\cos(-\frac{2}{3}\pi + 4\varepsilon_k) + 1\right)\Delta\theta_r\right\}\end{aligned} \qquad (22)$$

Therefore the condition for the estimation error ε to converge to zero at 5kHz sampling frequency becomes

$$\Delta V(k) < 0 \quad when \left\{\begin{array}{l} -30^\circ < \varepsilon_k < 60^\circ \\ 0rpm < \omega_r < 11937rpm \end{array}\right\} \qquad (23)$$

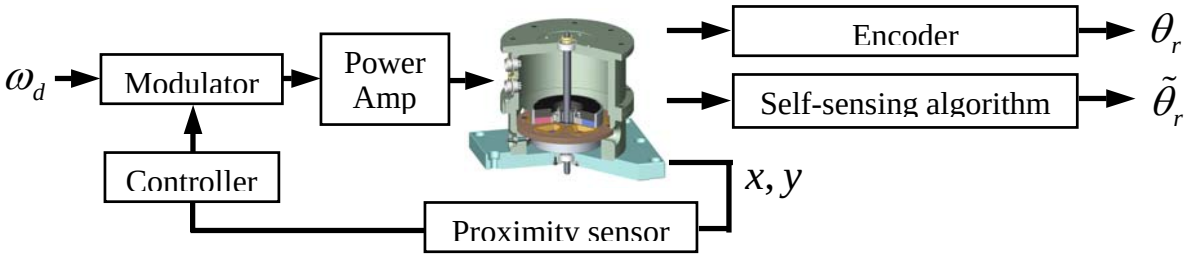

Fig. 5 Block diagram of experiment setup for self -sensing algorithm including direction control

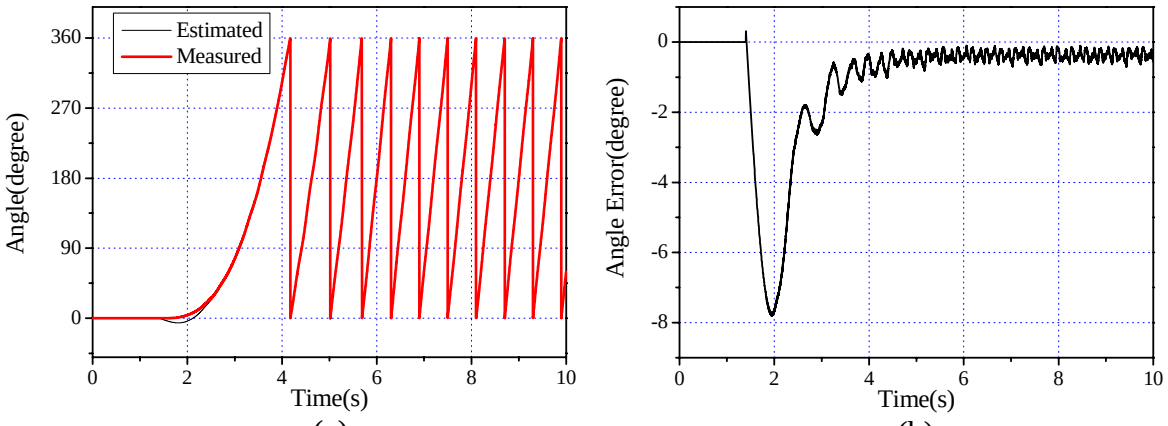

Fig. 6 (a) Measured and estimated angles and (b) angle estimation error: speed-up from 0 to 100 rpm with the rotor radial motion not allowed.

5. EXPERIMENT RESULTS

Figure 5 shows the overall configuration of the control loop in the experiment: an open loop control for speed control and a simple PD control for radial displacement control. The radial displacement signals of the rotor measured by a pair of proximity probes were fed into a DSP(dSPACE) through an A/D converter for the radial displacement control. A pair of control signals generated by the DSP was input to a power amplifier through a D/A converter, regulating the control currents to the stator windings. The estimated angular position of the rotor was then compared with the measured angles by the optical incremental encoder.

Figure 6 shows that the angle estimation error initially increased up to 8° and then converged nearly to zero (about 0.3°) within approximately 4 seconds, as the rotational speed was increased from 0 rpm to 100 rpm, while the radial motion of the rotor was not allowed. The results suggest that the proposed self-sensing algorithm can be applied even from the start-up state of the system, which is not normally expected from most of the previous angular position estimation methods based on back EMF.

Figure 7 shows the steady state angle estimation error at the constant rotational speed of 500 rpm with the rotor radial motion not allowed. As seen in Figs. 6 (b) and 7(b), the angle estimation error does not diverge even after a long lapse of time from the start-up, characterized by two types of error: the off-set and periodic errors. It is believed that the offset error results from the estimation error of flux linkage

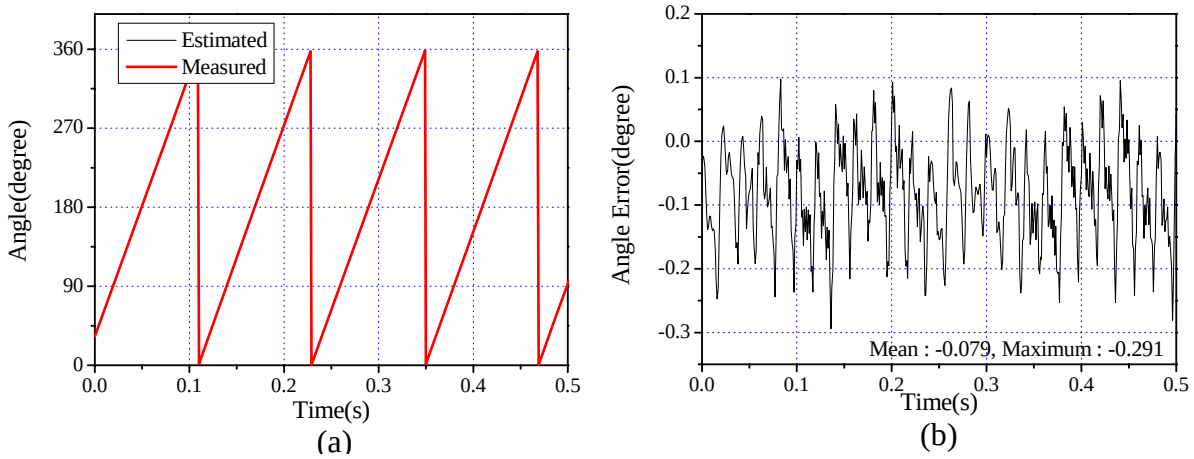

Fig. 7 (a) Measured and estimated angles and (b) angle estimation error: 500 rpm with the rotor radial displacement not allowed.

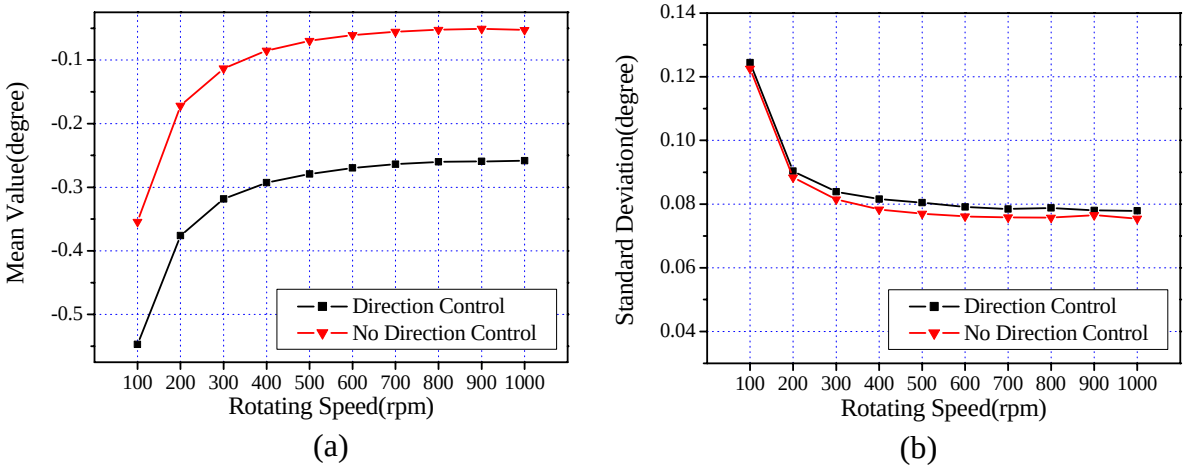

Fig. 8 (a) Mean value and (b) standard deviation of steady-state angle estimation error

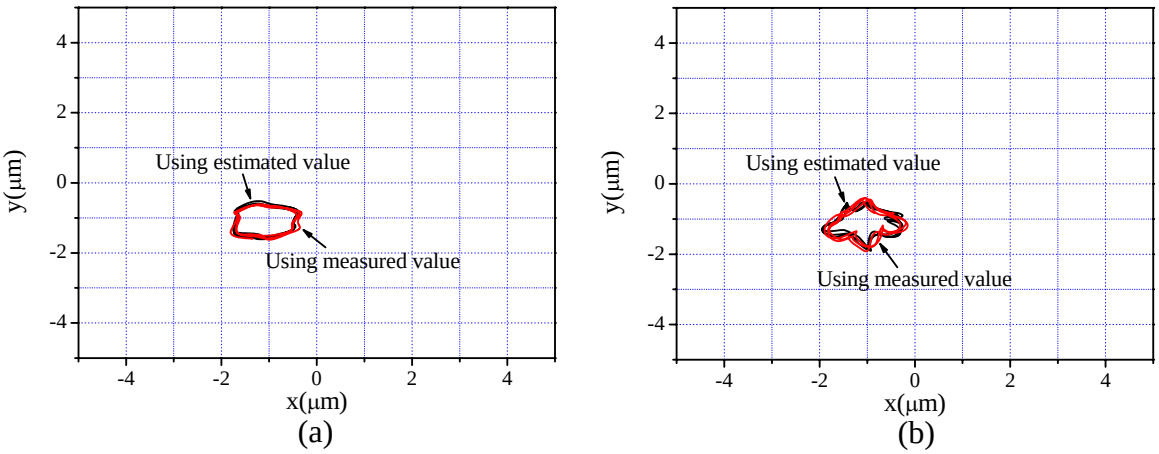

Fig. 9 Comparison of whirl orbits in rotor radial control (a) in the case of 100 rpm and (b) in the case of 500 rpm

due to the rotor eccentricity and the parameter uncertainty such as resistances, inductances, etc. The periodic error is due to the uneven magnetic flux distribution of the permanent magnets on the rotor, because the fundamental frequency of the periodic error is the six times the rotational speed, which is the same as the number of the stator windings.

As shown in equation (10), the proposed algorithm is independent of the radial displacement control currents. Figure 8 compares the mean and standard deviation of the angle estimation error over the speed range of 100 to 1000 rpm. Note that the error mean is larger for the radial displacement control, while the standard deviation is of the same magnitude. The maximum angle estimation error is not larger than 1° over the whole speed range of interest. Thus it can be concluded that the proposed simple algorithm (10) is very effective in estimation of the rotor rotation angle with fair accuracy.

Figure 9 compares two whirl orbits under the rotor radial control, one from feedback of the estimated angular position and another from measurement by the encoder. Note that there is little difference in control performance by two different methods.

CONCLUSIONS

In this paper, an angular self-sensing algorithm for the Lorentz force type IMB with six stator windings and eight rotor permanent magnets is proposed. It features that the absolute angular position of the rotor is estimated indirectly from calculation of flux linkages using the measured line voltages and currents to each stator winding. And the Lyapunov stability analysis proved that the angle estimation error converges to zero, in spite of the inherent integration form of the proposed algorithm. The experimental results show that the proposed algorithm can be applied even from the start-up state of the system, and the angle estimation error does not diverge for a sufficiently long lapse of time. It is also experimentally shown that the steady-state error mean decreases as the rotational speed increases, while the resolution of the angle estimation is kept less than 1° over the speed range up to 1000 rpm. The experimental results show that there is little difference in control performance between use of the estimated and measured angular positions for rotor radial control.

REFERENCES

1. Ueno, S., Chen, C., Ohishi, T., Matsuda, K., Okada, Y., Taenaka, Y., Masuzawa, T., Design of a Self-Bearing Slice Motor for a Centrifugal Blood Pump, 6th International Symposium on Magnetic Bearings, Cambridge, Massachusetts (1998) 143-151.

2. Salazar, A. O., Chiba, A., Fukao, T., A Review of Development in Bearingless Motors, 7th International Symposium on Magnetic Bearings, ETH, Zurich (2000) 335-340.
3. Okada, Y., Miyamoto, S., Ohishi, T., Levitation and Torque Control of Internal Permanent Magnet Type Bearingless Motor, *IEEE Transactions on Control System Technology*, Vol. 4, No. 5 (1996) 565-570.
4. Michioka, C., Sakamoto, T., Ichikawa, O., Chiba, A., Fukao, T., A Decoupling Control Method of Reluctance-Type Bearingless Motors Considering Magnetic Saturation, *IEEE Transactions on Industry Applications*, Vol. 32, No. 5 (1996) 1204-1210.
5. Chiba, A., Furuichi, R., Aikawa, Y., Shimada, K., Takamoto, Y., Fukao, T., Stable Operation of Induction-Type Bearingless Motors Under Loaded Conditions, *IEEE Transactions on Industry Applications*, Vol. 33, No. 4 (1997) 919-924.
6. Park, S. H., Lee, C. W., Design of Lorentz Force Type Integrated Motor-Bearing System Using Permanent Magnets and Concentrated Windings, *Proceedings of the 11th World Congress in Mechanism and Machine Science*, Tianjin, China (2003).
7. Okada, Y., Konishi, H., Kannebako, H., Lee, C. W., Lorentz Force Type Self-Bearing Motor," 7th International Symposium on Magnetic Bearings, ETH, Zurich (2000) 353-358.
8. French, C., Acarnley, P., Control of Permanent Magnet Motor Drives Using a New Position Estimation Technique, *IEEE Transactions on Industry Applications*, Vol. 32, No. 5 (1996) 1089-1097.
9. Ying, L., Ertugrul, N., A New Algorithm for Indirect Position Estimation in Permanent Magnet AC Motors, IEEE Power Electronics Specialists Conference (2002) 289-294.